

## Elastic scattering of neutrons from ${}^3\text{He}$ between 7.9 and 23.7 MeV\*

M. Drog,† D. K. McDaniels,‡ J. C. Hopkins, J. D. Seagrave, R. H. Sherman, and E. C. Kerr

*University of California, Los Alamos Scientific Laboratory, Los Alamos, New Mexico 87544*

(Received 27 September 1973)

Neutrons of 7.9, 12.0, 13.6, 14.4, and 23.7 MeV were elastically scattered from a 0.54-mole sample of liquid  ${}^3\text{He}$ . The angular distributions of the scattered neutrons were measured by the time-of-flight method at 14 angles ranging from  $\cos\theta_{\text{c.m.}} = 0.9$  to  $-0.7$  with relative errors of typically 4%. The absolute values were derived by comparison with the  ${}^1\text{H}(n,n){}^1\text{H}$  reaction with scale errors of about 3%. Many of the older distributions and total  $n$ - ${}^3\text{He}$  cross sections in this energy range are superseded by the new measurements. Upper limits for the  ${}^3\text{He}(n,np){}^2\text{H} + {}^3\text{He}(n,2n)2p$  cross-sections sum are derived. The differential cross sections at 7.9, 13.6, and 14.4 MeV are compared with their charge-symmetric counterpart at nearby energies. The contribution of this experiment to phase-shift analysis of the  ${}^3\text{He}(n,n){}^3\text{He}$  data is discussed.

NUCLEAR REACTIONS  ${}^3\text{He}(n,n){}^3\text{He}$ ,  $E = 7.9$ – $23.7$  MeV; measured  $\sigma(E;\theta)$ ; deduced  $\sigma_{\text{el}}$  and limits for  $\sigma_{\text{tot}}$  and  $\sigma_{n,2n} + \sigma_{n,pn}$ ; comparison with charge-symmetric reaction.

### I. INTRODUCTION

Experimental data on few-nucleon reactions are not only of practical value but needed also as background in theoretical few-nucleon investigations. Phase-shift analyses in the  ${}^4\text{He}$  system, the only  $A=4$  system with a bound state, have been used frequently to study the level structure of  ${}^4\text{He}$ .<sup>1</sup> These investigations were limited to lower energies<sup>2</sup> and restricted mainly to the reactions  ${}^3\text{H}(p,p){}^3\text{H}$  and  ${}^3\text{H}(p,n){}^3\text{He}$ .<sup>3</sup> A complete phase-shift analysis would have to treat all reaction channels simultaneously. In the case of the  ${}^4\text{He}$  system this is still a challenge due partly to the lack of experimental data on all reaction channels. Nevertheless, promising theoretical attempts have been made.<sup>4</sup> For the elastic  ${}^3\text{He}(n,n){}^3\text{He}$  channel only sparse experimental data were available and these results are inconsistent, as was shown by Drigo, Moschini, and Villi<sup>5</sup> and in a tentative phase-shift analysis of this reaction by Büsser and Niebergall.<sup>6</sup> Additional precise data on this reaction have long been needed to clarify this situation.

Angular distributions for  ${}^3\text{He}(n,n){}^3\text{He}$  were measured by Abramov,<sup>7</sup> Seagrave, Cranberg, and Simmons,<sup>8</sup> Sayres, Jones, and Wu,<sup>9</sup> and Antolković *et al.*<sup>10</sup>; polarizations for the same reaction have been reported by Seagrave, Cranberg, and Simmons,<sup>8</sup> Hollandsworth, Gilpatrick, and Bucher,<sup>11</sup> Behof, Hevezi, and Spalek,<sup>12</sup> Büsser *et al.*,<sup>13</sup> Busse *et al.*,<sup>14</sup> and recently by Lisowski.<sup>15</sup> Among the differential cross sections only the data at 1.0, 2.0, 2.7, 3.5, 5.0, and 6.0 MeV are not in contradiction with the present measurements.<sup>16</sup>

The new measurements were made with a sample of liquid  ${}^3\text{He}$ , utilizing the time-of-flight (TOF) method for energy selection of the scattered neutrons. As it is favorable for energy-independent phase-shift analyses to have differential cross-section data coinciding in energy with polarization data,<sup>6,17</sup> we chose energies of 7.9 and 12.0 MeV to match polarizations of Behof, Hevezi, and Spalek<sup>12</sup> and of Büsser *et al.*<sup>13</sup> The energy of 13.6 MeV was chosen to match the charge-conjugate reaction  ${}^3\text{H}(p,p){}^3\text{H}$  at this energy,<sup>18</sup> and 14.4 MeV was selected to supply the forward-angle branch for the distribution of Antolković *et al.*<sup>10</sup> Finally, 23.7 MeV was chosen as a high-energy point at which other few-nucleon data exist.<sup>17</sup>

### II. EXPERIMENTAL

#### A. Neutron production

Our experiment was performed at the Van de Graaff accelerator facility of the Los Alamos Scientific Laboratory (LASL). The data were taken at the neutron time-of-flight area of the High Voltage Engineering Corporation (HVEC) tandem accelerator utilizing a klystron buncher. Either protons or deuterons were bunched to provide the primary neutrons via the  ${}^3\text{H}(p,n){}^3\text{He}$  or the  ${}^3\text{H}(d,n){}^4\text{He}$  reactions. The cell for the tritium gas is described in Ref. 19. The deviation of the actual mean neutron energy from the nominal values of 7.90, 12.00, 13.60, 14.40, and 23.70 was less than 0.03 MeV in all cases. The energy spread [full width at half maximum (FWHM)] of

the primary neutron beam was 0.17 MeV at 7.9 MeV, less than 0.15 MeV at 12.0, 13.6, and 14.4 MeV, and 0.30 MeV at 23.7 MeV. This spread was due to the energy inhomogeneity of the charged-particle beam (finite-energy resolution of the accelerator, straggling in the entrance foil and in the gas of the target, and energy loss in the target) and the kinematic spread of the neutrons due to the finite solid angle subtended by the scattering sample. The time resolution (including contributions of the electronics) was typically less than 1.5 ns. The neutron flux was monitored by means of a detector which viewed the neutron source at  $110^\circ$  with respect to the beam line.<sup>20</sup> These results were crosschecked with the amount of accumulated charge as recorded by the beam current integrator.<sup>19</sup>

### B. Scattering sample

As in previous elastic scattering experiments at LASL involving the hydrogen and helium isotopes,<sup>16, 21, 22</sup> a liquid sample of the isotopically pure material was used, necessitating a cryostat for cooling the cell containing the  $^3\text{He}$ . The cylindrical cell had the same dimensions as in the earlier experiments (2.68 cm in diameter, 4.17 cm in height), providing 0.54 moles of  $^3\text{He}$  at a temperature of 2.85 K. (The cryogenic proper-

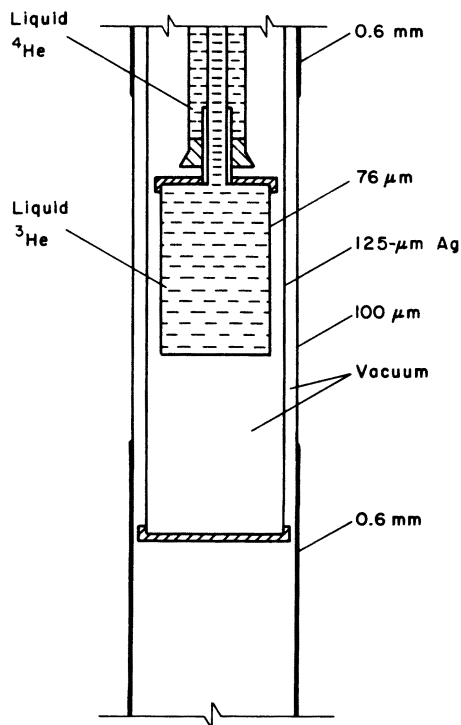


FIG. 1. Liquid  $^3\text{He}$  scattering sample cell.

ties of  $^3\text{He}$  are reviewed in Refs. 23–26.) This temperature was attained by pumping on the liquid-helium coolant. The coolant was in thermal contact with the filling tube of the cell (see Fig. 1), enabling the condensation of  $^3\text{He}$ . The advantage of a liquid sample (high density without high pressure) which allows the use of a container with thin walls was not so pronounced as in the previous experiments, because it was necessary to introduce, within the vacuum jacket, an additional heat shield made of a thin sheet of silver and maintained at liquid nitrogen temperature. Without this shield it was not possible to fill the cell with liquid  $^3\text{He}$ . For the same reason the liquid helium jacket cooling the filling tube had to approach the cell closely. Both provisions contributed considerably to the background.

The usual background run with a dummy cell was not enough to correct for the background because the dummy did not contain a coolant. Therefore a calculated correction for the in-scattering of  $(0.010 \pm 0.008)$  moles of liquid helium had to be applied.

Under these circumstances a gaseous sample is competitive with the liquid. This was shown at the end of our experiment, when we repeated three angles of our 12-MeV distribution using a gaseous sample. The same setup was used except for pumping on the coolant. At a temperature of 3.94 K the cell contained 0.225 moles of  $^3\text{He}$  gas. The disadvantage of the reduced mass was overcome by the precision of the background determination. After removing the gas from the cell, the cell itself could be used for the background run. This allowed direct correction for the contribution of the coolant and avoided systematic errors due to slight differences in the construction and in the positioning of the dummy and of the sample.

The construction of sample and dummy cells were compared by means of x-ray pictures. The cell positions were checked with the aid of a reference laser beam and a caliper. The distance from the center of the neutron target to the center of the sample was  $12.50 \pm 0.05$  cm.

### C. Time-of-flight setup

The neutron detector was a Nuclear Enterprises NE-213 liquid scintillator about 10 cm in diameter and with a sensitive length of 5.7 cm. Its relative efficiency as a function of energy was measured accurately.<sup>20</sup> The distance of the detector from the scattering sample was 256 cm. The shielding consisted of copper, lead, and polyethylene; the shadow bar was made of tungsten as described elsewhere.<sup>21, 22</sup> The angular position

of the detector was measured by means of a digitizer and was known to within  $\pm 0.1^\circ$ . The angular range was limited by the bulk of the collimator to angles less than  $119^\circ$ .

A simplified circuit diagram of the electronics is shown in Fig. 2. There are two independent TOF branches, one for the monitor detector and one for the main detector (M.D.). Start pulses for the time-to-amplitude converters (TAC) were derived from the fast signals of the photomultipliers, and stop pulses were obtained from the beam pickoff probe just before the target.  $n$ - $\gamma$  discrimination<sup>21</sup> reduced the background and dead time. The dead time of the main detector was determined by counting those bursts (stops) during which the electronics was busy. This type of dead-time correction requires a beam with no severe intensity changes within a time comparable to the dead time. The dead time of the monitor branch was typically less than 0.5% and was constant within  $\pm 0.1\%$  so that it was not corrected for.

The TOF spectra had about the same characteristics as in the  $^4\text{He}(n, n)^4\text{He}$  experiment (see Fig. 3 of Ref. 17), although the signal-to-background ratio was considerably smaller in the  $^3\text{He}$  case. This was due to the smaller cross section, the smaller number of scattering atoms in the sample, and the additional background from the heat shield and the coolant.

#### D. Procedure

The data for the angular distributions were collected in 11 sets of runs over a period of about

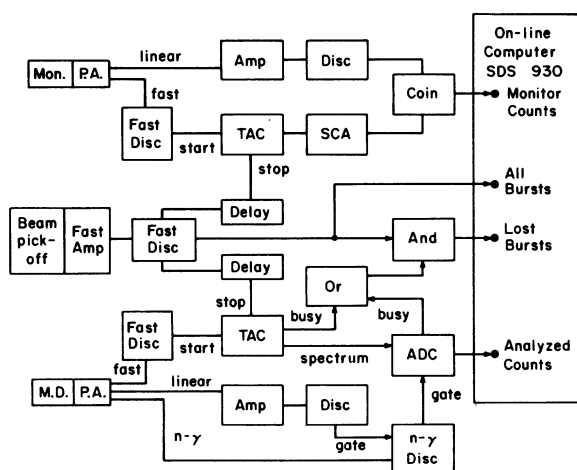


FIG. 2. Simplified circuit diagram. Mon. = monitor, P.A. = preamplifier, Amp = amplifier, Disc = discriminator, Coi = (slow) coincidence, TAC = time-to-amplitude converter, SCA = single-channel analyzer, M.D. = main detector.

half a year. The angles were so selected that the cosine of the corresponding center-of-mass angle was a multiple of 0.05.

Each data point comprises at least four measurements, done in the sample sequence IN, OUT, OUT, IN. The pulse-height discrimination bias in the linear branch of the main detector was set at a multiple of the Compton break of the 662-keV  $\gamma$  ray of  $^{137}\text{Cs}$  (symbolically  $k \times \text{Cs}$ ) and this setting was checked at intervals of eight hours at most. The bias level was so chosen that a good signal-to-background ratio could be expected without much loss of signal, i.e.,  $0.4 \times \text{Cs}$  for 7.9 MeV,  $1.0 \times \text{Cs}$  for 12, 13.6 and 14.4 MeV, and  $2.0 \times \text{Cs}$  for 23.7 MeV.

After normalization to the same neutron monitor counts and after background correction by combining corresponding sample-in and sample-out runs, the raw data contained in the TOF peak were corrected for the energy dependence of the detector efficiency corresponding to the pulse-height bias employed (see Fig. 4 of Ref. 20). These corrected yields were then converted into absolute differential cross sections by comparing them with the similarly corrected yield of a scattering measurement from the cross-section standard.

As our standard we used the cross sections of the reaction  $^1\text{H}(n, n)^1\text{H}$  as calculated using the Yale phase shifts.<sup>27</sup> These cross-section values were compared with the yields of elastic scattering from hydrogen in a polyethylene plate at an angle near  $40^\circ$  and at the same primary neutron energy as used in the  $n$ - $^3\text{He}$  scattering. Details such as the attenuation correction in the slab are discussed in Ref. 20. The use of slabs instead of cylinders in the standard measurements (with all the advantages discussed in Ref. 20) does not introduce detectable errors. This was shown by comparing the yields of the flat polyethylene sample with that of a hollow cylinder with the same outside dimensions as the  $^3\text{He}$  sample. They agreed within the statistical error of 0.5%.

#### III. DATA AND ERROR DISCUSSION

The absolute differential cross sections derived as described in the previous section had to be corrected for neutron flux attenuation and multiple scattering in the sample. The latter was done with a Monte Carlo Code MAGGIE-2 adopted for a CDC 7600 computer from the AWRE version.<sup>28</sup> The cross-section library necessary as input for this code containing originally all previous data on the  $n$ - $^3\text{He}$  reaction, was changed after a first iteration incorporating our new corrected results and deleting unreliable older cross sections. Multiple scattering changed the shape of the dis-

TABLE I. Lab cross sections for the reaction  ${}^3\text{He}(n, n){}^3\text{He}$  in mb (liquid samples only).

Energy $\cos\theta_{c.m.}$	7.00 MeV		12.00 MeV		13.60 MeV		14.40 MeV		23.70 MeV	
	$\theta_{lab}$	$\sigma \pm \Delta\sigma$	$\theta_{lab}$	$\sigma \pm \Delta\sigma$	$\theta_{lab}$	$\sigma \pm \Delta\sigma$	$\theta_{lab}$	$\sigma \pm \Delta\sigma$	$\theta_{lab}$	$\sigma \pm \Delta\sigma$
0.90	19.4	620. $\pm$ 39.	19.5	537. $\pm$ 18.	19.4	471. $\pm$ 17.	19.3	436. $\pm$ 15.	19.4	267. $\pm$ 12.
0.80	27.9	496. $\pm$ 25.	28.0	415. $\pm$ 18.	27.9	345. $\pm$ 13.	27.7	341. $\pm$ 11.	27.8	194. $\pm$ 7.
0.70	34.5	421. $\pm$ 13.	34.6	301. $\pm$ 7.	34.6	273. $\pm$ 9.	34.5	265. $\pm$ 9.	34.6	140. $\pm$ 6.
0.60	40.5	320. $\pm$ 10.	40.5	228. $\pm$ 8.	40.5	209. $\pm$ 7.	40.5	189. $\pm$ 7.	40.5	96.8 $\pm$ 5.4
0.55	43.4	274. $\pm$ 11.	43.4	195. $\pm$ 5.	43.4	172. $\pm$ 4.	43.4	166. $\pm$ 5.	43.4	76.1 $\pm$ 3.5
0.40	51.2	186. $\pm$ 8.	51.3	121. $\pm$ 8.	51.4	106. $\pm$ 4.	51.4	104. $\pm$ 4.	51.3	47.4 $\pm$ 3.2
0.25	58.8	109. $\pm$ 5.	58.9	75.2 $\pm$ 4.7	58.8	69.2 $\pm$ 2.8	58.8	66.2 $\pm$ 2.6	58.9	28.1 $\pm$ 1.7
0.10	66.4	66.5 $\pm$ 3.3	66.4	44.9 $\pm$ 2.5	66.5	36.9 $\pm$ 1.8	66.3	33.0 $\pm$ 1.8	66.3	17.6 $\pm$ 1.5
0.00	71.4	42.4 $\pm$ 1.9	71.6	27.8 $\pm$ 1.1	71.6	24.6 $\pm$ 1.1	71.4	23.7 $\pm$ 1.0	71.5	10.5 $\pm$ 1.9
-0.10	76.5	29.1 $\pm$ 1.3	76.8	17.6 $\pm$ 1.3	76.8	17.0 $\pm$ 1.0	76.6	14.3 $\pm$ 0.8	76.6	7.44 $\pm$ 0.86
-0.30	87.9	15.7 $\pm$ 0.8	87.8	7.53 $\pm$ 0.39	87.8	6.26 $\pm$ 0.31	87.8	6.08 $\pm$ 0.35	87.8	5.50 $\pm$ 0.72
-0.50	100.8	17.7 $\pm$ 1.2	100.9	7.31 $\pm$ 0.52	100.8	5.94 $\pm$ 0.32	100.7	5.06 $\pm$ 0.33	100.7	4.10 $\pm$ 0.73
-0.60	108.4	22.3 $\pm$ 1.3	108.4	11.4 $\pm$ 0.7	108.4	8.53 $\pm$ 0.44	108.5	7.84 $\pm$ 0.36	108.3	4.33 $\pm$ 0.55
-0.715	118.3	29.7 $\pm$ 1.2	118.2	16.7 $\pm$ 1.0	118.5	12.4 $\pm$ 0.7	118.5	12.3 $\pm$ 0.46	118.5	5.46 $\pm$ 0.58
Scale errors (not included)		$\pm 3.1\%$		$\pm 2.8\%$		$\pm 3.1\%$		$\pm 2.8\%$		$\pm 2.9\%$

tributions up to about 10%. The typical effect of the multiple-scattering correction on the angular distribution is illustrated in Fig. 4 of Ref. 17. The flux attenuation correction took into account both the cryostat and the sample itself. It decreased from about 5.0% at 7.9 MeV to 2.6% at 23.7 MeV.

The values for the differential cross section after all corrections had been applied are tabulated in Table I. The errors include all contributions affecting the shape of the distributions except for errors in the multiple-scattering correction, in dead-time correction, and in the stability of pulse-height discrimination.

The error in the dead-time correction (estimated to be less than 0.5%) is negligible. Changes in the pulse-height discrimination bias (primarily due to gain changes of the photomultiplier) affect the results only slightly if the neutron energy is high compared to the equivalent proton energy of the bias. The energy of the backmost scattered neutrons (the worst case) was about 2.5 times the bias energy for all five sets. The effect of any percentage shift of the bias was therefore reduced. Errors due to unnoticed shifts were thought to be less than 1% and were not included. The error for the multiple-scattering correction is less than 1% for the point with the largest correction (assuming a 10% precision of the correction), and when added quadratically is practically negligible. In addition, systematic errors in the background subtraction were not accounted for except for the error in calculating the coolant contribution to the background (see Sec. IIB).

The error in the relative efficiency was assumed to be  $\pm 1.5\%$  per 10 MeV for energies below 12 MeV and  $\pm 2.5\%$  per 10 MeV for energies below 22 MeV.<sup>20</sup> This error does not enter in the scale of the cross section but affects the shape only. Obviously that point of the distribution which coincides in energy with the energy of the cross-section standard comparison has no efficiency error of this kind. With increasing difference in energy the error increases. Therefore, instead of a uniform efficiency error as was assumed in Ref. 17, an individual error was assigned to each point.

A compilation of all these errors and the scale errors is given in Table II. Energy-independent systematic contributions to the scale errors include uncertainties in the number of scattering nuclei ( $\leq \pm 0.5\%$  for the hydrogen standard and  $\pm 1.4\%$  for the  ${}^3\text{He}$  sample). For all runs equal errors were assumed for the precision of the standard ( $\leq \pm 0.5\%$ ), for differences of the geometry ( $\leq \pm 1\%$ ), and for the flux-attenuation and multiple-scattering corrections for the standard measurement ( $\leq \pm 0.8\%$ ). All the other errors

TABLE II. Sources of errors.

Individual (shape) errors	Scale errors
Statistical uncertainties	(a) Connected with the standard:
Normalization	Precision of standard cross section
Background subtraction	Mass of standard sample: purity, weight
Energy dependence of detector efficiency	Statistical uncertainties
Multiple-scattering correction	Normalization (neutron dose)
Dead-time correction	Background subtraction
Detector bias stability	Flux attenuation and multiple scattering
	Dead-time correction
	Difference in geometry
	(b) Connected with the sample:
	Mass: purity, volume, density (vapor pressure)
	Flux attenuation

were taken into account individually for each data set. The total scale errors are shown in Table I.

Toward the end of the experiment it was decided to remeasure some cross sections with a gaseous sample in order to reduce systematic errors as discussed in Sec. II B, and thus to improve the knowledge of the absolute scale. Three angles at 12 MeV were chosen to be duplicated (see Table III). Aside from reduced errors in the background subtraction, affecting the shape errors, a scale error smaller than in the liquid case was achieved (2.4% compared to 2.8%). This was due to reduced errors in the attenuation correction, in the normalization, and in the number of counts. The uncertainties connected with the reference cross section and with the volume of the sample were common to both measurements.

It was assumed that the gas was in thermal equilibrium with the coolant and that any deviation from this condition did not alter the gas density by more than 1%.

As shown in Table III the agreement between the two measurements is extremely good. A combination of the two (partly dependent) results allows establishing an even better scale for the 12.00-MeV differential cross sections than that given in Table I. The two scales agree to a factor  $1.001 \pm 0.010$ , obtained from the three ratios in Table III. This allows reduction of the final scale error for the 12.00-MeV distribution to 2.3%. The three duplicated differential cross sections were obtained with high accuracy, as shown in the last column. The errors shown do not include any scale errors. Although all other sources of

TABLE III. Comparison between liquid and gaseous  $^3\text{He}$  samples at 12.00 MeV (lab cross sections in mb).

$\cos\theta_{c.m.}$	Liquid	Gas	Combined <sup>a</sup>	Ratio liquid: combined	Combined
0.70	301. $\pm$ 7.	295. $\pm$ 5.	297. $\pm$ 4.	1.013 $\pm$ 0.026	297. $\pm$ 4.
0.60	228. $\pm$ 8.	232. $\pm$ 4.	232. $\pm$ 3.	0.986 $\pm$ 0.037	232. $\pm$ 4.
0.55	195. $\pm$ 5.	198. $\pm$ 3.	197. $\pm$ 2.	0.991 $\pm$ 0.028	197. $\pm$ 3.
Scale errors:					
in common	1.5%	1.5%			1.5%
individual	2.3%	1.9%			1.8%
total	2.8%	2.4%			2.3%

<sup>a</sup> Independent errors only.

errors were included in these numbers (and only independent errors had been combined quadratically), the errors are so close to the lower limit for this apparatus that previously neglected systematic errors might play a role.

#### IV. COMPARISON WITH PREVIOUS DATA AND WITH CHARGE SYMMETRIC DATA

Our results were compared with previous angular distributions,<sup>9, 10</sup> with previous<sup>29</sup> and new<sup>30</sup> total cross sections, and with distributions of the charge-symmetric reaction  ${}^3\text{H}(p, p){}^3\text{H}$ .<sup>18, 31</sup> Our 7.90-MeV data are at nearly the same energy as the 8.07-MeV distribution of Sayres, Jones, and Wu.<sup>9</sup> There is a pronounced disagreement (of up to 30%) between these older data and ours (see Fig. 3). Also the 17.5-MeV distribution of Sayres, Jones, and Wu,<sup>9</sup> which is of poor statistical quality, deviates seriously beyond  $80^\circ(\text{c.m.})$  from our (interpolated) distribution for this energy. We conclude, therefore, that the higher-energy recoil-counter measurements of Sayres, Jones, and Wu suffer from undetected systematic errors, which may affect their 2.67- and 5.00-MeV data as well.

To agree with the present measurements, the backward-angle distribution of Antolković *et al.*<sup>10</sup> (see Fig. 4), which is given with statistical errors only, should be lowered by about 10%; whereas their single point at  $180^\circ$ , which was measured in an earlier experiment,<sup>32</sup> should be raised by about 25%. Systematic errors in these results would explain the difficulties Büsser and Niebergall<sup>6</sup> had with these data when using them for a phase-shift analysis.

As pointed out by Baz,<sup>33</sup> cross sections of charge-

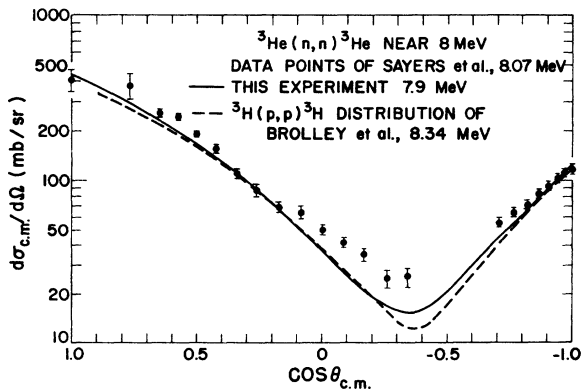


FIG. 3. Comparison of present results (full line) at 7.90 MeV with the data of Sayres, Jones, and Wu (Ref. 9) at 8.07 MeV (points), and with the charge-symmetric  ${}^3\text{H}(p, p){}^3\text{H}$  data of Brolley *et al.* (Ref. 35) at 8.34 MeV (broken line).

symmetric reactions should not be compared at the same total energy but at the same energy of nuclear interaction. This is done, e.g., by Hardekopf, Walter, and Clegg,<sup>34</sup> when comparing  ${}^2\text{H}(d, p){}^3\text{H}$  with  ${}^2\text{H}(d, n){}^3\text{He}$  data at the same energy of the outgoing particle (neglecting Coulomb effects).

In the  ${}^3\text{H}(p, p){}^3\text{H}$  reaction the Coulomb repulsion reduces the incoming proton energy by approximately 0.5 MeV.<sup>4</sup> As the differential cross sections do not change rapidly with energy, we neglect small energy differences in the following qualitative comparisons and do not correct for the Coulomb interaction. Figure 5 compares our  ${}^3\text{He}(n, n){}^3\text{He}$  results at 13.60 MeV with those of Detch *et al.*<sup>18</sup> at the same energy. The resemblance both in scale and shape is striking. In Fig. 3 our 7.90-MeV distribution is compared with the 8.34-MeV distribution of Brolley *et al.*<sup>35</sup> and in Fig. 4 our 14.40-MeV distribution with the 14.6-MeV distribution of Rosen and Leland.<sup>31</sup> Comparing all three pairs of charge-symmetric differential cross sections one finds the following features: The absolute scale and the general tendency of the shape agree very well. On the other hand, there is an indication of a systematic difference which is common to all three distribu-

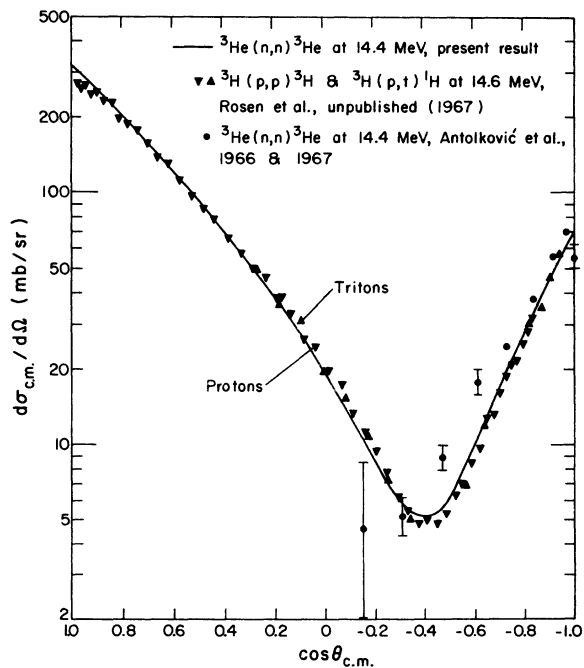


FIG. 4. Comparison of present results (full line) at 14.40 MeV with those of Antolković *et al.* (Refs. 10 and 32) at 14.4 MeV (full circles) and with the charge-symmetric  ${}^3\text{H}(p, p){}^3\text{H}$  and  ${}^3\text{H}(p, t){}^1\text{H}$  data of Rosen and Leland (Ref. 31) at 14.6 MeV (triangles).

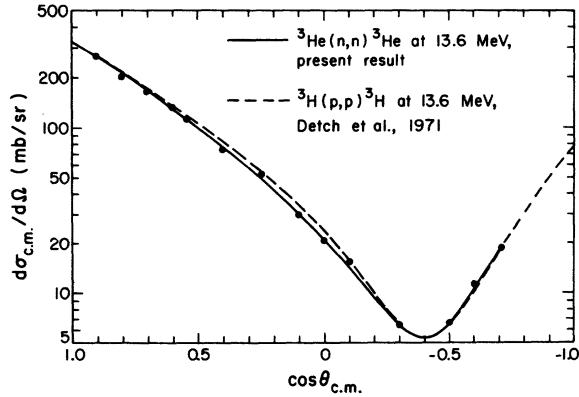


FIG. 5. Comparison of present results (full line and dots) at 13.60 MeV with the charge-symmetric  $^3\text{H}(p,p)^3\text{H}$  data of Detch *et al.* (Ref. 18) at the same energy (broken line).

tions. At forward angles (for  $\cos\theta_{\text{c.m.}} > 0.5$ ) the  $n$ - $^3\text{He}$  distribution is steeper; for angles with cosines between 0.2 and  $-0.2$  the  $p$ - $^3\text{H}$  distribution appears to be steeper.

This good general agreement with the charge-symmetric reaction and the very good agreement of the backward-angle  $n$ - $^3\text{He}$  distribution of Seagrave, Cranberg, and Simmons<sup>8</sup> at 6.0 MeV with

TABLE IV.  $n$ - $^3\text{He}$  integral and elastic  $0^\circ$  differential cross sections (in barns).

Type	$E_n$ (MeV)	7.90	12.00	13.60	14.40	23.70
$\sigma_T^a$		1.78	1.30	1.17	1.12	0.70
		$\pm 0.018$	$\pm 0.020$	$\pm 0.035$	$\pm 0.035$	$\pm 0.055$
$\sigma_{\text{el}}(0^\circ)_{\text{Wick}}^b$		0.43	0.35	0.32	0.31	0.20
$\sigma_{\text{el}}(0^\circ)^{b,c}$		0.44	0.36	0.34	0.33	0.22
$\sigma_{\text{el}}^d$		1.43	1.04	0.92	0.87	0.48
		$\pm 0.05$	$\pm 0.03$	$\pm 0.03$	$\pm 0.03$	$\pm 0.02$
$\sigma_{\text{ne}} = \sigma_T - \sigma_{\text{el}}$		0.35	0.26	0.25	0.25	0.22
		$\pm 0.05$	$\pm 0.04$	$\pm 0.05$	$\pm 0.05$	$\pm 0.06$
$\sigma_{n,p}^e + \sigma_{n,d}^f$		0.31	0.24	0.23	0.22	0.15 <sup>c</sup>
		$\pm 0.01$	$\pm 0.01$	$\pm 0.01$	$\pm 0.02$	$\pm 0.02$
$\sigma_{n,pn} + \sigma_{n,2n}$		0.04	0.02	0.02	0.03	0.07
		$\pm 0.05$	$\pm 0.04$	$\pm 0.05$	$\pm 0.05$	$\pm 0.06$

<sup>a</sup> Data of Ref. 30.

<sup>b</sup> Barns/steradian.

<sup>c</sup> Extrapolated.

<sup>d</sup> By integration.

<sup>e</sup> Converted data of D. K. McDaniels, M. Drogg, J. C. Hopkins, and J. D. Seagrave, Phys. Rev. C **6**, 1593 (1972).

<sup>f</sup> Adjusted from data of: J. E. Brolley, Jr., T. M. Putnam, and L. Rosen, Phys. Rev. **107**, 821 (1957); M. D. Goldberg and J. M. Leblanc, Phys. Rev. **119**, 1992 (1960); and W. T. H. Van Oers and K. W. Brockmann, Nucl. Phys. **48**, 625 (1963).

that of Brolley *et al.*<sup>35</sup> at 6.5 MeV for the  $p$ - $^3\text{H}$  reaction suggested using the corresponding  $p$ - $^3\text{H}$  shapes to complete our  $n$ - $^3\text{He}$  distributions from  $\cos\theta_{\text{c.m.}} = -0.715$  to  $\cos\theta_{\text{c.m.}} = -1.00$  (see Fig. 6). In this figure the arrows pointing to the  $\cos\theta = 1.00$  axis denote Wick's limits, as derived from the optical theorem using the total  $n$ - $^3\text{He}$  cross section, to give lower limits for the  $0^\circ$  cross sections. Our extrapolated  $0^\circ$  cross sections were not above Wick's limit when using literature values<sup>29</sup> for the total cross sections. The sums of the integrated differential elastic and the non-elastic cross sections were also lower than the published total values. Therefore a remeasurement of the total cross sections was suggested

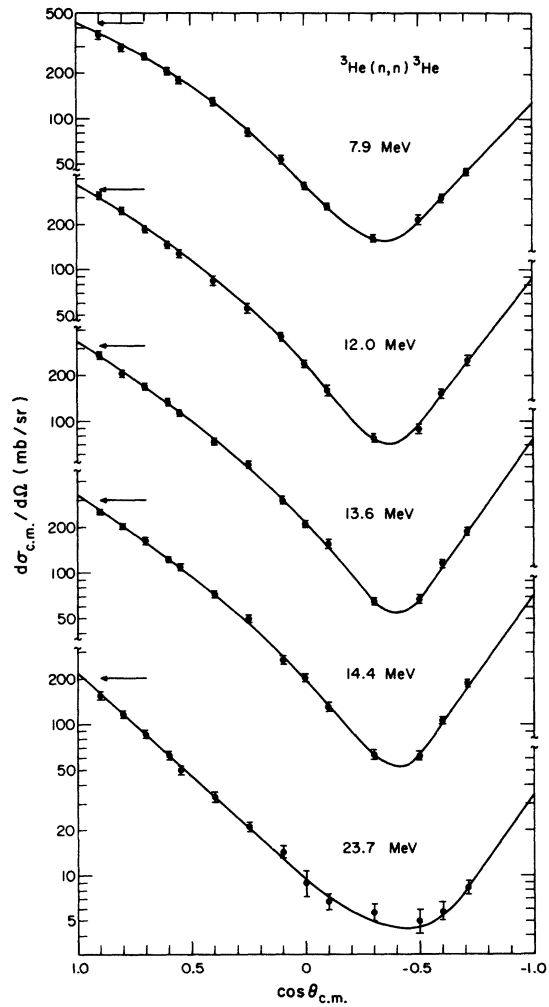


FIG. 6. Present c.m. angular distributions at 7.90, 12.00, 13.60, 14.40, and 23.70 MeV. Backward-angle dependence of curves were taken from corresponding  $^3\text{H}(p,p)^3\text{H}$  distributions. Wick's limits shown by arrows were calculated with total cross sections from Ref. 30.

after our measurements with the gas had confirmed our absolute scale. The new values for the total cross section obtained at Rensselaer Polytechnic Institute<sup>30</sup> are in good agreement with our data (see Table IV). Thus Wick's limit was used as an indirect check on the total cross section. The possibility of errors in the total cross section which enter quadratically in Wick's limit is often overlooked, as, e.g., by Drigo, Moschini, and Villi<sup>5</sup> in their check of the  ${}^3\text{He}(n, n){}^3\text{He}$  distribution at 6.0 MeV.<sup>8</sup> Table IV summarizes various partial cross sections for the  $n$ - ${}^3\text{He}$  reaction. The total elastic cross section  $\sigma_{el}$  was obtained by integration of the distributions giving absolute values which are tied to the  ${}^1\text{H}(n, n){}^1\text{H}$  cross section. The difference between the total and the integral elastic cross section comprises the non-elastic cross section  $\sigma_{ne}$ . The difference between  $\sigma_{ne}$  and the sum of the cross sections for the  ${}^3\text{He}(n, p){}^3\text{H}$  and the  ${}^3\text{He}(n, d){}^2\text{H}$  reactions is due to the unobserved  ${}^3\text{He}(n, pn){}^2\text{H}$  and the  ${}^3\text{He}(n, 2n)2p$  breakup reactions. Thus predictions for these reactions could be made in this table.

#### V. DISCUSSION AND CONCLUSION

The comparison of our differential cross sections with previous data suggests that there may exist serious systematic errors in the data of Sayres, Jones, and Wu<sup>9</sup> and of Antolković *et al.*<sup>10, 32</sup> There then remain eight reliable distributions between 1 and 14.4 MeV, and one at 23.7 MeV which allows interpolations up to this energy. The close agreement with the charge-conjugate reaction which is demonstrated for energies up to 14.4 MeV suggests use of the  ${}^3\text{H}(p, p){}^3\text{H}$  data at 16.23 and 19.48 MeV<sup>18</sup> to bridge the gap between 14.4 and 23.7 MeV. They should not differ at any angles by more than about  $\pm 10\%$  from their neutron counterpart (disregarding very forward

angles). For the spin-dependent cross sections the situation looked much less favorable until the very recent polarization work of Lisowski.<sup>15</sup> Aside from his new measurements at 8.0, 12.0, and 17.1 MeV, only the distributions at 3.0 MeV<sup>11</sup> and 16.0 MeV<sup>13</sup> seem to be useful. In addition, there are a few points at 1.1 and 2.2 MeV.<sup>8</sup> All the other polarization data (at 3.3,<sup>12</sup> 7.9,<sup>12</sup> 12.0,<sup>13</sup> and 21.9 MeV<sup>14</sup>) are either in direct disagreement with more recent and precise data or in disagreement with the phase-shift analysis by Lisowski.<sup>15</sup> This phase-shift analysis made use of our data as well. Its solutions give excellent fits to our cross-section data and the new polarization results, and predict integrated and  $0^\circ$  cross sections which are very close to those of Table IV. The previous, tentative analysis of Büsser and Niebergall<sup>6</sup> relied mainly on the superseded data of Sayres, Jones, and Wu.<sup>9</sup> At forward angles their solutions deviate by about 20% from our measurement (at 12 MeV). Also, Busse *et al.*<sup>14</sup> found their results in disagreement with Büsser's analysis.

The impact of the new data on the integral cross sections was unexpected. They not only led to a remeasurement of the total cross sections for the  $n$ - ${}^3\text{He}$  reactions,<sup>30</sup> but they also allow placing limits on the breakup cross sections as shown in Table IV. However, only at 23.7 MeV is the sum  $\sigma_{n, pn} + \sigma_{n, 2n}$  inconsistent with zero. These data are also in agreement with the only other datum (at 14.1 MeV) on the  $n, 2n$  reaction<sup>36</sup> [ $\sigma_{n, 2n} = (1 \pm 11)$  mb].

#### ACKNOWLEDGMENTS

We thank J. T. Martin for his help with the setup and during the runs. The staff of the LASL Tandem Accelerator Facility contributed considerably to the success of this experiment.

\*Work performed under the auspices of the U. S. Atomic Energy Commission.

†On leave from the University of Vienna, Vienna, Austria. Present address: First Phys. Institute, A-1090 WIEN, Austria.

‡On leave from the University of Oregon, Eugene, Oregon 97403.

<sup>1</sup>W. E. Meyerhof and T. A. Tombrello, Nucl. Phys. **A109**, 1 (1968).

<sup>2</sup>W. E. Meyerhof and J. N. McElearney, Nucl. Phys. **74**, 533 (1965).

<sup>3</sup>C. Werntz and W. E. Meyerhof, Nucl. Phys. **A121**, 38 (1968).

<sup>4</sup>P. Szydlik and C. Werntz, Phys. Rev. **138**, B866 (1965).

<sup>5</sup>L. Drigo, G. Moschini, and C. Villi, Nuovo Cimento,

**49B**, 227 (1967).

<sup>6</sup>F. W. Büsser and F. Niebergall, in *Few Body Problems, Light Nuclei, and Nuclear Interactions*, edited by G. Paić and I. Šlaus (Gordon and Breach, New York, 1968), p. 469 ff.

<sup>7</sup>A. I. Abramov, Zh. Exp. Teor. Fiz. **37**, 1476 (1959) [transl.: Sov. Phys.—JETP **10**, 1046 (1960)].

<sup>8</sup>J. D. Seagrave, L. Cranberg, and J. E. Simmons, Phys. Rev. **119**, 1981 (1960).

<sup>9</sup>A. R. Sayres, K. W. Jones, and C. S. Wu, Phys. Rev. **122**, 1853 (1961).

<sup>10</sup>B. Antolković, G. Paić, P. Tomaš, and D. Rendić, Phys. Rev. **159**, 777 (1967).

<sup>11</sup>C. E. Hollandsworth, M. Gilpatrick, and W. P. Bucher, Phys. Rev. **C 5**, 395 (1972).



- <sup>12</sup>A. F. Behof, J. M. Hevezi, and G. Spalek, Nucl. Phys. 84, 290 (1966).
- <sup>13</sup>F. W. Büsser, H. Dubenkropp, F. Niebergall, and K. Sinram, Nucl. Phys. A129, 666 (1969).
- <sup>14</sup>W. Busse, B. Efken, D. Hilscher, H. Morgenstern, and J. A. Scheer, Nucl. Phys. A187, 21 (1972).
- <sup>15</sup>P. W. Lisowski, Ph.D. thesis, Duke University, 1973 (unpublished); and private communication.
- <sup>16</sup>M. Drog, D. K. McDaniels, J. C. Hopkins, J. D. Seagrave, and E. C. Kerr, Bull. Am. Phys. Soc. 16, 829 (1971).
- <sup>17</sup>A. Niler, M. Drog, J. C. Hopkins, J. D. Seagrave, and E. C. Kerr, Phys. Rev. C 4, 36 (1971).
- <sup>18</sup>J. L. Detch, Jr., R. L. Hutson, N. Jarmie, and J. H. Jett, Phys. Rev. C 4, 52 (1971).
- <sup>19</sup>D. K. McDaniels, I. Bergqvist, D. Drake, and J. T. Martin, Nucl. Instrum. Methods 99, 77 (1972).
- <sup>20</sup>M. Drog, Nucl. Instrum. Methods 105, 573 (1972).
- <sup>21</sup>J. D. Seagrave, J. C. Hopkins, R. K. Walter, A. Niler, P. W. Keaton, Jr., E. C. Kerr, and R. H. Sherman, Ann. Phys. (N. Y.) 74, 250 (1972).
- <sup>22</sup>J. D. Seagrave, in *Few Body Problems, Light Nuclei, and Nuclear Interactions*, edited by G. Paić and I. Šlaus (Gordon and Breach, New York, 1968), p. 787 ff.
- <sup>23</sup>R. H. Sherman, S. G. Sydoriak, and T. R. Roberts, NBS J. Res. 68A/6, 579 (1964).
- <sup>24</sup>E. C. Kerr and R. D. Taylor, Ann. Phys. (N. Y.) 20, 450 (1962).
- <sup>25</sup>R. M. Gibbons and C. McKinley, Adv. Cryo. Eng. 13, 375 (1968).
- <sup>26</sup>J. G. Daunt and D. O. Edwards, Ann. Rev. Phys. Chem. 15, 83 (1964).
- <sup>27</sup>J. C. Hopkins and G. Breit, Nucl. Data A9, 137 (1971).
- <sup>28</sup>J. B. Parker, J. H. Towle, D. Sams, W. B. Gilboy, A. D. Purnell, and H. J. Stevens, Nucl. Instrum. Methods 30, 77 (1964).
- <sup>29</sup>Los Alamos Physics and Cryogenics Groups, Nucl. Phys. 12, 291 (1959).
- <sup>30</sup>C. A. Goulding, P. Stoler, and J. D. Seagrave, Rensselaer Polytechnic Institute Technical Report No. COO-3058-27 (1972); and private communication.
- <sup>31</sup>L. Rosen and W. T. Leland, unpublished; numerical values are given in Idaho Nuclear Corp. Report No. WASH-1079, 1967 (unpublished).
- <sup>32</sup>B. Antolković, M. Cerineo, G. Paić, P. Tomaš, V. Adjacić, B. Lalović, W. T. H. Van Oers, and I. Šlaus, Phys. Lett. 23, 477 (1966).
- <sup>33</sup>A. I. Baz, Zh. Exp. Teor. Fiz. 32, 478 (1957) [transl.: Sov. Phys.-JETP 5, 403 (1957)].
- <sup>34</sup>R. A. Hardekopf, R. L. Walter, and T. B. Clegg, Phys. Rev. Lett. 28, 760 (1972).
- <sup>35</sup>J. E. Brolley, Jr., T. M. Putnam, L. Rosen, and L. Stewart, Phys. Rev. 117, 1307 (1960).
- <sup>36</sup>D. S. Mather and L. F. Pain, United Kingdom Atomic Energy Research Establishment Report No. AWRE 0-47/69; and private communication.